Environ Earth Sci (2016) 75:1374
DOI 10.1007/s12665-016-6160-x

THEMATIC ISSUE

Investigating the age distribution of fracture discharge using multiple environmental tracers, Bedrichov Tunnel, Czech Republic

W. Payton Gardner[1] · Milan Hokr[2] · Hua Shao[3] · Ales Balvin[2] · Herbert Kunz[3] · Yifeng Wang[4]

Received: 28 February 2016 / Accepted: 3 October 2016 / Published online: 19 October 2016

Abstract The transit time distribution (TTD) of discharge collected from fractures in the Bedrichov Tunnel, Czech Republic, is investigated using lumped parameter models and multiple environmental tracers. We utilize time series of $\delta^{18}O$, δ^{2}H and ^{3}H along with CFC measurements from individual fractures in the Bedrichov Tunnel of the Czech Republic to investigate the TTD, and the uncertainty in estimated mean travel time in several fracture networks of varying length and discharge. We compare several TTDs, including the dispersion distribution, the exponential distribution, and a developed TTD which includes the effects of matrix diffusion. The effect of seasonal recharge is explored by comparing several seasonal weighting functions to derive the historical recharge concentration. We identify best fit mean ages for each TTD by minimizing the error-weighted, multi-tracer χ^2 residual for each seasonal weighting function. We use this methodology to test the ability of each TTD and seasonal input function to fit the observed tracer concentrations, and the effect of choosing different TTD and seasonal recharge functions on the mean age estimation. We find that the estimated mean transit time is a function of both the assumed TTD and seasonal weighting function. Best fits as measured by the χ^2 value were achieved for the dispersion model using the seasonal input function developed here for two of the three modeled sites, while at the third site, equally good fits were achieved with the exponential model and the dispersion model and our seasonal input function. The average mean transit time for all TTDs and seasonal input functions converged to similar values at each location. The sensitivity of the estimated mean transit time to the seasonal weighting function was equal to that of the TTD. These results indicated that understanding seasonality of recharge is at least as important as the uncertainty in the flow path distribution in fracture networks and that unique identification of the TTD and mean transit time is difficult given the uncertainty in the recharge function. However, the mean transit time appears to be relatively robust to the structural model uncertainty. The results presented here should be applicable to other studies using environmental tracers to constrain flow and transport properties in fractured rock systems.

Keywords Environmental isotopes · Hydrogeology · Isotope geochemistry · Surface water · DECOVALEX

This article is part of a Topical Collection in Environmental Earth Sciences on "DECOVALEX 2015", guest edited by Jens T Birkholzer, Alexander E Bond, John A Hudson, Lanru Jing, Hua Shao and Olaf Kolditz.

✉ W. Payton Gardner
payton.gardner@umontana.edu

[1] Department of Geosciences, University of Montana, 32 Campus Dr #1296, Missoula, MT, USA

[2] Technical University of Liberec, Studentska 2, 46117 Liberec, Czech Republic

[3] Federal Institute for Geosciences and Natural Resources, Stilleweg 2, 30655 Hanover, Germany

[4] Sandia National Laboratories, 1515 Eubank Blvd SE, Albuquerque, NM, USA

Introduction

Flow and transport in fracture networks remains one of the more challenging issues facing hydrogeologists today. Accurate predictions of flow and transport in fracture networks are important in a variety of hydrogeologic problems including: nuclear waste repository safety assessment,

contaminant transport and remediation, unconventional hydrocarbon production, enhanced geothermal energy production and mine reclamation. Fractured reservoirs are characterized by extreme heterogeneity and data scarcity. Generally, it is not possible to uniquely determine the spatial distribution of fracture network properties and provide a complete description of the system behavior; however, simple models which incorporate field data at the appropriate scale should be able to provide insight into the salient feature of the system behavior (Neuman 2005). The transport time distribution is a powerful description of the flow and transport in a hydrogeologic system; however, little is known about the field scale transit time distribution in fracture networks. Lumped parameter models provide a simplified methodology to investigate the residence time distribution in fracture networks.

Transport in fracture networks is affected by rapid advection in fractures and diffusion into and out of adjacent intact lower-permeability matrix (e.g., Haggerty et al. 2001; Maloszewski and Zuber 1985, 1990; Neretnieks 1980; Sudicky and Frind 1982; Tang et al. 1981). The effect of matrix diffusion is to slow tracer transport compared to the advective fluid velocity, dampen concentration variation and produce long tailing of tracer release (Cook and Robinson 2002; Maloszewski and Zuber 1985; Neretnieks 1980, 1981). Tracer transport in fractured networks has been evaluated theoretically and used to interpret tracer transport experiments with a variety of models from analytical models of simple geometry to numerical models of discrete fracture networks. Multiple continuum models allow linear exchange between the advective and immobile porosities for a single rate (Warren and Root 1963) to multiple mass transfer rates (Haggerty and Gorelick 1995). Analytical solutions exist for models that account for concentration gradients in the matrix for simple geometries such as a single fracture (Tang et al. 1981), parallel fractures (e.g., Maloszewski and Zuber 1985, 1990; Sudicky and Frind 1982) and a distribution of different matrix block shapes and sizes (e.g., Haggerty et al. 2000). Discrete fracture network models have been used to develop fully distributed reactive flow and transport models (e.g., Therrien and Sudicky 1996) as well as produce fluid velocity fields for particle tracking schemes which can be post-processed to account for matrix interactions (e.g., Painter and Cvetkovic 2005; Painter et al. 2008; Roubinet et al. 2013). The parameters used in these models are a strong function of the spatial and temporal scale of interest (Neuman 2005; Shapiro 2001); thus, observations used to estimate fracture parameters should be made at similar length and time scales to the desired predictions.

Environmental tracers can provide a rich dataset which can be used to understand fracture flow and transport over a wide range of spatial and temporal scales. Environmental tracer concentrations have been used to develop conceptual models of tracer transport and constrain fracture network parameters in a variety of fractured rock systems. Cook and Robinson (2002) develop an analytical model of environmental tracer transport in parallel fractures and show that tracer concentrations could not uniquely determine fracture network properties, but were capable of providing some constraint fracture spacing, aperture and recharge. Cook et al. (2005) use this model to constrain the recharge rate in a fractured, porous aquifer in South Australia, and show that this simple model was a reasonable representation of a more complex system and could be used to predict concentration breakthrough.

Groundwater mean age can be used to characterize the residence time distribution in fracture networks. Analytical models of mean groundwater age have been developed in fractured systems (Doyon and Molson 2012). Groundwater age in the field is often determined using environmental tracer concentrations. However, in fracture networks, environmental tracer concentrations provide the solute residence time, which is not equal to the advective residence time (Neretnieks 1981). Thus, "apparent" groundwater ages determined from environmental tracers will be older than the advective fluid residence time (Cook and Robinson 2002), and the use groundwater age in fractured systems must incorporate matrix interactions.

The residence time distribution is a fundamental characteristic of a flow system and provides critical information for determining the parameters controlling flow and transport in the system. Residence time distributions have been developed for a variety of simplistic aquifers (Cook and Herczeg 2000; Maloszewski and Zuber 1996). These models provide a convenient method to investigate the residence time and flow path distribution in hydrogeologic systems (e.g., Gardner et al. 2010, 2011; Solomon et al. 2010, 2015). Lumped parameter models in conjunction with tracer transport observations provide a means to investigate the residence time distribution and infer flow path characteristics in a reservoir (Danckwerts 1953). Multiple environmental tracers can be used to identify the best age distribution and mixing models which best fit the observed data (Gardner et al. 2011; Solomon et al. 2010). McCallum et al. (2014) show that age tracers have limited ability to uniquely identify the age distribution, but indicate the time series of tracers can help reduce uncertainty. Solomon et al. (2010) indicate that the mean ages derived from multiple environmental tracers appear to be robust to the choice of the transit time distribution. However, these studies were carried out for porous flow aquifers and the application of lumped parameter models in fractured flow systems to estimate the transit time distribution is questionable.

The aim of this paper is to provide some insight into the uncertainty in estimating the mean transit time and the ability to distinguish the transit time distribution in fracture networks discharging to single fractures at the scale of 100s of meters using lumped parameter models and multiple environmental tracer concentrations. We utilize time series of $\delta^{18}O$, $\delta^{2}H$ and ^{3}H along with CFC measurements from individual fractures in the Bedrichov Tunnel of the Czech Republic (Fig. 1) to investigate the TTD in several fracture networks of varying length and discharge. We compare several transit time distributions, including a developed TTD which includes the effects matrix diffusion. We identify best fit mean ages for each TTD and compare the ability of each TTD to fit the observed tracer concentrations and the effect of choosing different TTDs on the mean age estimation.

Theory

Lumped parameter models were developed to investigate residence time distributions in chemical reactors where the true distribution of flow paths is not known (Danckwerts 1953). The breakthrough curve of a tracer transported through the reactor can be used to provide information on the distribution of flow paths, and the processes affecting transport in the reactor, for example, the amount of dead volume, the degree of mixing, and the amount of dispersion in 1D flow in the reactor (Danckwerts 1953). The residence time distribution has been used to investigate flow and transport in groundwater systems where the exact distribution of flow paths is unknown for many decades (e.g., Maloszewski and Zuber 1996). The concentration at time t is given by the convolution integral:

$$C(t) = \int_0^\infty C_{\text{in}}(t - t')g(t')e^{-\lambda t}\mathrm{d}t', \quad (1)$$

where t' is the residence time, λ is the decay constant of a radioactive tracer, $C(t - t')$ is the historical input at recharge and $g(t')$ is the residence time distribution for the flow paths discharging to the sampling point. Equation 1 along with observations of tracer concentration in groundwater allows for the investigation of the distribution of flow paths and the processes affecting transport in the "black box" flow system which feeds the discharge point.

Residence time distribution

The residence time distribution contains the flow and transport information for the system upstream of the sampling point and has been derived for several simplified aquifer types (Cook and Herczeg 2000; Maloszewski and Zuber 1996). Here we consider two existing transit time distributions which encompass two possible end members of reservoir types, and develop a distribution which incorporates matrix diffusion. The simplest age distribution considered is for water flowing along a single flow path or fracture subject to longitudinal dispersion, termed here as the dispersion distribution which can be written (Maloszewski and Zuber 1982):

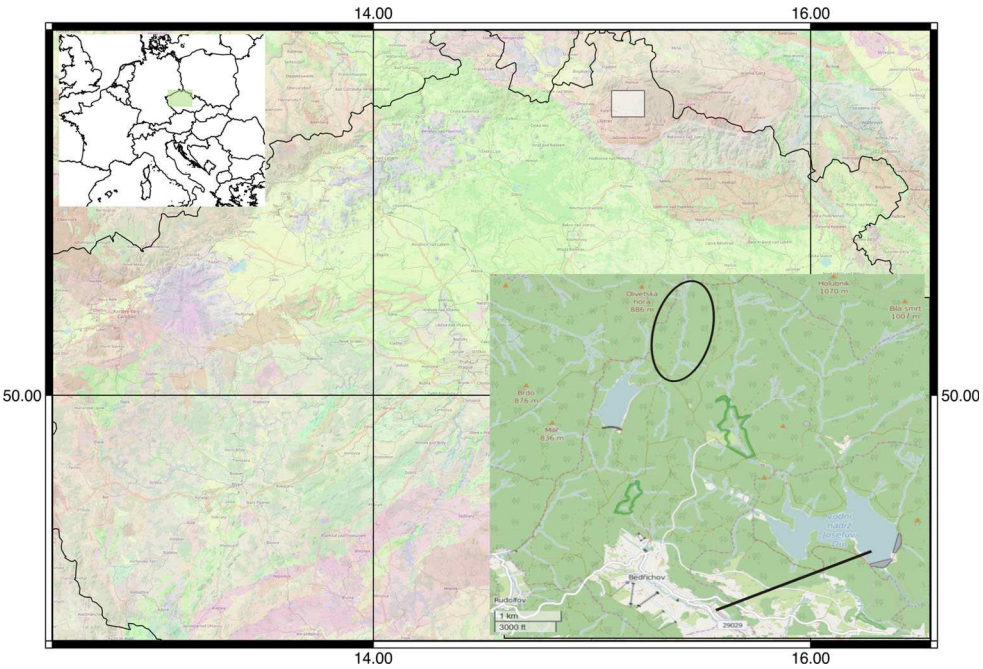

Fig. 1 Map of the Bedrichov Tunnel location. Surface geology is overlain on the mid-scale location map. The *red coloring* at the Bedrichov site represents the granite batholith. Bedrichov Tunnel location marked by *black line*. Uhlirska experimental watershed marked with oval in fine scale *inset*

$$g(t') = t'^{-1}(4\pi P_e t'/\tau)^{-1/2}\exp\left[\frac{-\tau * (1-t'/\tau)^2}{4P_e t'}\right], \quad (2)$$

where $P_e = D/vx$ is the system Peclet number with longitudinal dispersivity D, velocity v and transport distance x, and τ is the mean transit time.

An exponential distribution of residence times is achieved when there is complete mixing of flow paths of all ages, thus representing an end member where many different flow paths converge to the sampled fracture. The exponential distribution is written (Maloszewski and Zuber 1982):

$$g(t') = \frac{1}{\tau}e^{-\frac{t'}{\tau}}. \quad (3)$$

Equations 2 and 3 were developed for porous media aquifers and do not consider the effect of diffusion into immobile regions on the transit time. In this study, a transit time distribution is developed that includes the effects infinite matrix diffusion for a constant fracture aperture. Here, we assume that the diffusion time to equilibrate matrix blocks with the fracture fluid is long compared to the changes in concentration and that the fracture system is uniform.

The total transport time distribution ($g_{\text{tran}}(t_{\text{tran}})$) can be written as the convolution of the advective travel time distribution $g(t')$ and the retention time distribution ($g_{\text{ret}}(t_{\text{ret}})$) coupled by a velocity-dependent transport-resistant parameter distribution (Painter et al. 2008):

$$g_{\text{tran}}(t_{\text{tran}}) = \int_0^{\infty}\int_0^{t_{\text{tran}}} g_{\text{ret}}(t_{\text{tran}} - t'|\beta) f_{\beta|t'}(\beta|t') g(t')\mathrm{d}t'\mathrm{d}\beta, \quad (4)$$

where $t_{\text{tran}} - t' = t_{\text{ret}} \geq 0$ is the retention time from matrix diffusion and β is the spatially variable velocity-dependent transport resistance parameter with a density distribution of $f_{\beta|t'}(\beta|t')$. If variability in the resistance parameter is neglected (Painter et al. 2008):

$$f_{\beta|t'}(\beta|t') = \delta(\beta - t'\bar{\beta}/\tau) \quad (5)$$

where δ is the Dirac function. In fractured rock applications, the resistance parameter is defined (Painter et al. 2008):

$$\beta(t') = \int_0^{t'} \frac{ds}{b(s)}, \quad (6)$$

where b is the fracture half aperture and s is distance along the flow path. If a constant aperture is assumed, then (Painter et al. 2008):

$$\beta = \frac{t'}{\bar{b}} = t'\frac{\bar{\beta}}{\tau}, \quad (7)$$

where $\bar{b}$ is the effective fracture aperture for the system of interest.

Painter et al. (2008) present retention time distributions for a wide variety of subsurface transport processes. For this paper, unlimited matrix diffusion is considered. The retention time distribution for infinite matrix diffusion is:

$$g_{\text{ret}}(t_{\text{ret}}|\beta) = \frac{\kappa\beta}{2\sqrt{\pi}t_{\text{ret}}^{3/2}}\exp\left[\frac{-\kappa^2\beta^2}{4t_{\text{ret}}}\right], \quad (8)$$

where $\kappa = \theta_{\text{im}}\sqrt{D_{\text{im}}}$ is a function of the matrix porosity θ_{im} and the matrix diffusion coefficient D_{im}.

The concentration at time t for a system which includes matrix diffusion can now be written:

$$C(t) = \int_0^{\infty} C_{\text{in}}(t - t_{\text{tran}}) g_{\text{tran}}(t_{\text{tran}})\mathrm{d}t_{\text{tran}}. \quad (9)$$

Inserting Eqs. 4 into 9 and assuming constant aperture and no variance in the resistance transport parameter (Eqs. 7 and 5) give:

$$C(t) = \int_0^{\infty} C_{\text{in}}(t - t_{\text{tran}})\int_0^{t_{\text{tran}}} g_{\text{ret}}(t_{\text{tran}} - t'|\beta)(t'/\bar{b})g(t')\mathrm{d}t'\mathrm{d}t_{\text{tran}}. \quad (10)$$

Equation 10 describes the transit time distribution and the resulting concentration expected in fracture discharge at time t and is a function of the purely advective travel time, modified by retention from diffusion into the adjacent matrix. Here, flow along a single constant aperture fracture is considered; thus, the advective travel time is assumed to the dispersion distribution (Eq. 2). Equation 10 is then parameterized by the mean advective travel time τ, the longitudinal dispersivity P_e, the fracture aperture $\bar{b}$, matrix porosity θ_{im} and diffusivity D_{im}.

Seasonal input function

The concentration input history $C_{\text{in}}(t)$ in Eqs. 1 and 10 is the historical concentration of a given tracer in water recharging the aquifer system. The concentration of these tracers is generally measured in precipitation and/or the atmosphere. The concentration in recharge will be modified from the atmospheric or precipitation concentration by the processes occurring during recharge such as soil flow, evapotranspiration and seasonality of precipitation. When recharge is constant throughout the year, C_{in} will be equal to the concentration in precipitation. However, in cases where the concentration of the tracer changes seasonally, seasonality in precipitation, infiltration or evapotranspiration can cause C_{in} to differ from the atmospheric or precipitation record. The annual flux weighted average concentration of tracer ($C_{\text{in}_{\text{an}}}$) is given by:

$$C_{\text{in}_{\text{an}}} = \frac{\sum_{i=1}^{12} C_i \alpha_i P_i}{\sum_{i=1}^{12} \alpha_i P_i}, \tag{11}$$

where $\alpha_i = R_i/P_i$ the recharge fraction is fraction of precipitation which become recharge for the ith month. In the area of the Bedrichov Tunnel, winter is wetter and colder with precipitation predominantly falling as snow and is a time of low evapotranspiration potential. During the summer months, precipitation falls as rain and there is a high evapotranspiration potential; thus, there is a significant potential for seasonality in the recharge function.

To investigate the effects of seasonality, we split the year into two seasons—summer and winter—and assume constant recharge fractions for summer months (α_s) and winter months (α_w). If the seasonal infiltration ratio $\alpha = \alpha_s/\alpha_w$ is defined, the seasonal recharge can be approximated by (Grabczak et al. 1984; Zuber and Maloszewski 2001):

$$C_{\text{in}_{\text{an}}} = \frac{\left(\alpha \sum_{i=4}^{9} C_i P_i\right)_s + \left(\sum_{i=10}^{3} C_i P_i\right)_w}{\left(\alpha \sum_{i=4}^{9} P_i\right)_s + \left(\sum_{i=10}^{3} P_i\right)_w}, \tag{12}$$

where the summer months are assumed to be April through October and winter months November through March. The mean stable isotope composition of groundwater can be used to estimate α:

$$\alpha = \frac{\left(\sum_{i=3}^{10} P_i \delta_i\right)_w - \delta\left(\sum_{i=3}^{10} P_i\right)_w}{\delta\left(\sum_{i=4}^{9} P_i\right)_s - \left(\sum_{i=4}^{9} P_i \delta_i\right)_s}, \tag{13}$$

where δ is the mean groundwater isotope composition and sums are calculated for all winter and summer months on record.

The long-term seasonal infiltration ratio α can now be used to estimate the seasonally weighted composition of recharge. This estimate has been done in variety of manners. The simplest and most common method is to use Eq. 12 to calculate the seasonally weighted annual average concentration. However, this limits the temporal resolution of the input function to annual steps. Interpretation of the high-resolution isotopic composition could provide information at sub-annual timescales, requiring a higher resolution input function. In this paper, seasonally weighted annual average precipitation along with three plausible monthly resolution input functions is investigated. The first and simplest high-resolution input function is simply the precipitation record, which inherently assumes $\alpha = 1$. The second infiltration function, taken from Zuber and Maloszewski (2001), is:

$$\delta_{\text{in}}(t) = \bar{\delta} + \alpha_i P_i (\delta_I - \bar{\delta}) / \sum_{i=1}^{12} \alpha_i P_i / n, \tag{14}$$

where $\bar{\delta}$ is the mean input (which must equal the mean output) and $\alpha_i = 1$ when $10 \geq i \leq 3$ and $\alpha_i = \alpha$ otherwise. We also develop another weighting function very close in form to Eq. 14:

$$\delta_{\text{in}}(t) = \bar{\delta} + \alpha_i P_i (\delta_I - \bar{\delta}) / \sum_{i=1}^{12} \alpha_i P_i. \tag{15}$$

The subtle difference between Eqs. 14 and 15 is in the normalization term. Equation 14 is normalized by the average monthly recharge; thus, recharge events greater than the average monthly recharge have much larger isotope shifts; however, this results in large fluctuations of the isotope composition when the precipitation is above the monthly average and probably underestimates mixing in the vadose zone. Conversely, Eq. 15 is normalized by the total annual precipitation, which means that only months which comprise a significant amount of the total seasonally weighted total annual recharge can cause deviation from the seasonally weighted annual average recharge. This function produces a very smooth infiltration function very close to the seasonally weighted average concentration, but does allow large precipitation events to modify the input signal.

It is important to note that seasonality is only important when the concentration of a tracer changes seasonally. Thus, seasonality is especially important for stable isotopes of water and tritium. For dissolved gases such as CFCs and SF_6, the concentration is set by the recharge temperature and excess air, which may not change appreciably seasonally; thus, seasonality may not be as important for these tracers.

Study area

The study location is a water supply tunnel which connects Josefuv Dul Reservoir with a water processing plant through a portions of the Jizera Mountains in the northern Czech Republic (Fig. 1). A description of the site can be found in Hokr et al. (DECOVALEX 2015 at http://www.decovalex.org/resources.html#special-issues). The tunnel is excavated through crystalline granitic rocks of the Krkonose–Jizera Composite Massif, a part of the Bohemian Massif of central Europe. The 2600-m tunnel was excavated in 1980–1981 with a maximum depth 150 m below land surface (Fig. 2). The tunnel has been utilized as a natural analogue underground laboratory for understanding fracture flow by the Czech Radioactive Waste Repository

Authority (SURAO), since 2003 (Klomínský and Woller 2010).

Detailed geological history of the massif and characterization of the fracture network intersecting the tunnel are given in Zak et al. (2009). The $\sim$1000 km^2 Krkonose–Jizera Plutonic Complex is dominated by the Jizera and Liberec coarse-grained porphyritic granodiorite to granite. The tunnel lies in the Jizera granite which is crosscut by two sets of steeply dipping roughly orthogonal fracture sets trending NE–SW and NW–SE. Fractures are roughly planar and sub-parallel and show little interaction with each other. Fracture spacing ranges from 1 cm to several meters with the most common spacing between 10 and 120 cm. Most fractures do not transmit measurable water discharge.

Fracture discharge and isotopic composition data were collected by the Technical University of Liberec and Czech Technical University in Prague respectively from 2010 to 2014 as part of the SURAO characterization project and IAEA Coordinated Research Project CZ16335. These data were made available as part of the DECOVALEX 2015 project as part of a task to model flow and transport in fractured crystalline systems. Historical isotope composition of precipitation is available from the Uhlirska experimental watershed, isotopes in precipitation database (Šanda et al. 2014).

Field and analytical methods

Measurements of the fracture discharge, water quality and temperature were taken at the sampling locations depicted in Fig. 2. The irregularly spaced sampling intervals were chosen to be representative of different flow regimes in the tunnel (Fig. 2). Manual measurements of fracture discharge were taken at each site at 14-day intervals starting in 2006. Fracture discharge was measured using V-notch weirs or drip counting, depending on the fracture discharge. Automatic measurements of fracture discharge at hourly intervals began in 2009 (Rálek and Hokr 2013). The locations of automatic measurement have continuously expanded since 2009; thus, the density of data and sampling intervals vary for each sampling site. Automated measurements are verified by manual measurements at the 14-day intervals.

Stable isotope composition of fracture discharge at the sampling sites has been measured since 2010. Stable isotope samples were collected at 14-day intervals in 50-ml bottles and analyzed at the Czech Technical University in Prague (CTU) by laser adsorption spectrometry (Penna et al. 2010). Dissolved CFCs, tritium and dissolved noble gases were measured at the IAEA Isotope Hydrology Laboratory as part of an IAEA Technical Cooperation Project (Research Contract CZ16335) and in Faculty of Science, Charles University in Prague. Dissolved CFCs were collected in 250 ml glass bottles with metal caps completely submerged in buckets filled with fracture discharge. Dissolved CFC concentrations were measured using purge and trap gas chromatography. Tritium was collected in L 1 bottles and analyzed by electrolytic enrichment and counting. Dissolved noble gases were collected using copper tube samples (Weiss 1968) and analyzed using mass spectrometry.

Modeling methods

The input concentration history $C_{\text{in}}(t)$ was estimated at the site for each tracer modeled. Stable isotopes in precipitation near the study site are available from the Uhlirska experimental watershed (Fig. 1) at monthly intervals beginning in 2006. The Vienna stable isotope in precipitation data set, the closest and longest time series in the IAEA Global Network of Isotopes in Precipitation, was used to provide an estimate of the values in precipitation at the site from 1960 to 2006.

The seasonal recharge coefficient α was calculated for each modeled location using the average δD and $\delta^{18}O$ composition measured in the groundwater samples and the

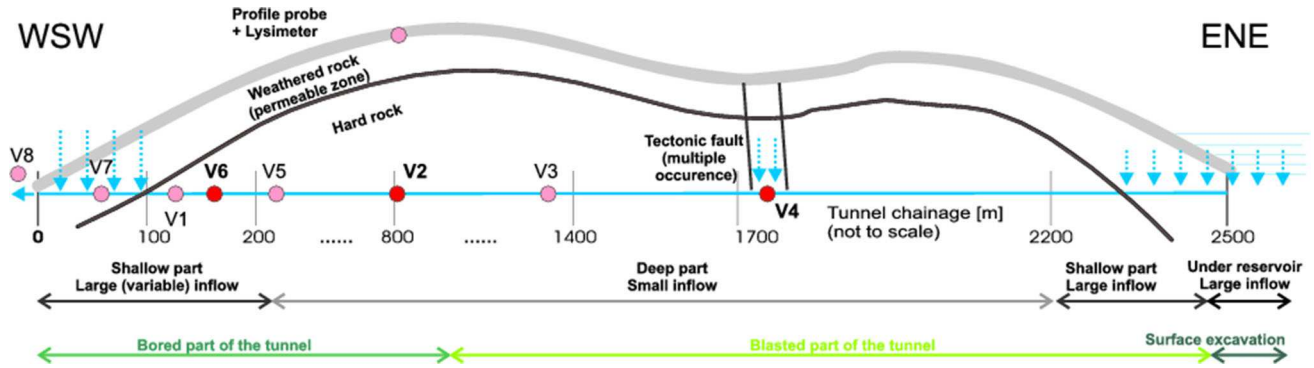

Fig. 2 Schematic cross section and profile of the Bedrichov Tunnel along with technical and hydrological conditions

average of Uhlirska precipitation dataset and using Eq. 13 to calculate an α for each isotope. The α used to create the seasonally weighted recharge concentration was taken as the average of that calculated for each isotope. Seasonally weighted concentrations were then calculated for tritium, δD and $\delta^{18}O$ using raw historical precipitation and Eqs. 12, 14 and 15 for each sampling site at monthly intervals. The precipitation record and the seasonal weighting functions are shown in Fig. 3. The input history for CFCs was calculated using the historical CFC mixing ratios in the atmosphere (Bullister 2011), the average noble gas recharge temperature estimate of 4.8 °C from noble gas concentration made as part of the IAEA tritium–helium analyses, a characteristic recharge elevation of 750 m, and zero excess air, to give the CFC concentration at each site in biannual intervals. We assume that the noble gas recharge temperature does not change appreciably over the seasonal cycle; thus, the CFC input time series does not change seasonally. In order to provide high enough temporal resolution to reduce numerical error, the time was resampled at daily intervals using linear interpolation to give the discrete concentration input history $\bar{C}_{\text{in}}$.

Equations 1–10 were simulated using discrete convolution of linearly interpolated concentration input history ($\bar{C}_{\text{in}}$) and weighting function vectors ($\bar{g}$). Numerically efficient discrete convolution was accomplished using multiplication of the Fourier transformed discrete vectors. Convolution operations were written in python.

Three of the sampling locations depicted in Fig. 2 representative of: shallow high discharge (V6), deep low-discharge fracture discharge (V2), and deep large discharge (V4) were modeled. The concentration in discharge was modeled at each location using Eq. 1 with the dispersion and exponential weighting functions and 10 with the dispersion advective travel time distribution. At each modeled location, three different concentration input histories were evaluated (Eqs. 12, 14 and 15) using the methods described above.

For each combination of weighting function and historical concentration history, the best fit mean groundwater age at a sampling site was estimated by fitting the observed multi-tracer data at the site. Best fit estimation was accomplished by minimizing error-weighted chi-squared residual for all tracers simultaneously at all sampling times using a Levenberg–Marquardt algorithm. The error in the mean age estimate was calculated from the 95 % confidence interval of the covariance matrix, using the Jacobian of the error-weighted chi-squared residual.

Results

The best fit modeled age, uncertainty estimate and χ^2 fit are reported for each precipitation weighting function for each age distribution at all modeled fracture locations in Tables 1 and 2. At each location, the mean age and standard deviation in estimated age for each age distribution due to the different conceptualization of seasonal recharge function is summarized in Table 4. The mean age and the standard deviation in mean age estimates due to the assumed age distribution is reported for each input function in Table 5. The effect of increasing mean travel time on δ^{18}O signal, along with the observed values at the V6 sampling site, is shown for a dispersion TTD (Eq. 2), using

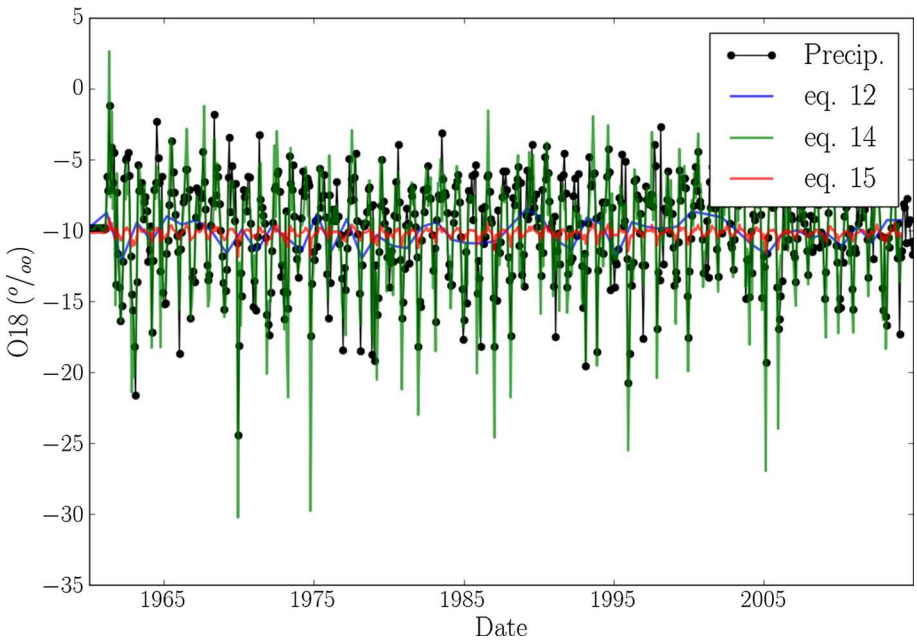

Fig. 3 Time series of $\delta^{18}O$ in precipitation at the Uhlirska site, and for each infiltration weighting function discussed

Table 1 Summary results for V6 sampling site

Age distribution ($g(t)$)	Infil. func. ($C_{in}(t)$)	τ_{adv} (years)	+/− (years)	χ^2	τ_{tran} years
Dispersion-matrix diffusion	Uniform	2.31	0.09	573	4.73
	Eq. 11	3.09	0.31	299	6.67
	Eq. 14	2.62	0.15	240	5.49
	Eq. 15	2.19	0.65	200	4.45
Dispersion	Uniform	2.65	0.1	343	–
	Eq. 11	7.17	0.73	283	–
	Eq. 14	2.58	0.15	189	–
	Eq. 15	1.27	0.14	177	–
Exponential	Uniform	3.1	0.18	651	–
	Eq. 11	5.64	0.44	328	–
	Eq. 14	5.78	0.55	382	–
	Eq. 15	5.5	0.46	317	–

Table 2 Summary results for V2 sampling site

Age distribution ($g(t)$)	Infil. func. ($C_{in}(t)$)	τ_{adv} (years)	+/− (years)	χ^2	τ_{tran} years
Dispersion-matrix diffusion	Uniform	2.57	0.13	575	5.37
	Eq. 11	4.56	0.32	214	10.6
	Eq. 14	2.83	0.2	272	6.03
	Eq. 15	3.22	1.95	107	6.99
Dispersion	Uniform	3.13	0.14	445	
	Eq. 11	8.22	0.93	202	
	Eq. 14	7.32	1.07	250	
	Eq. 15	6.65	5.4	108	
Exponential	Uniform	3.07	0.18	466	
	Eq. 11	7.72	0.7	226	
	Eq. 14	6.66	0.77	303	
	Eq. 15	6.81	6	111	

the annual average weighted precipitation function (Eq. 11) as shown in Fig. 4. As the age increases, the variation in the $\delta^{18}O$ signal decreases. The corresponding effect on the CFC-12 concentration along with observed data for the V6 sampling site is shown in Fig. 5. During the multi-tracer inversion, the difference between all the observed tracer and the modeled signal is minimized by varying the mean transit time.

Table 1 gives the summarized results for the V6 sampling site. The overall mean age for all age distributions and all recharge weighting functions is 4.58 years with a σ of 1.02 years. For the dispersive age distribution, the mean estimated age over all input functions is 3.4 years with a standard deviation (σ) of 2.6 years. The exponential age distribution gives a mean age of 5.0 years with a σ of 1.28 years for all input functions. For the matrix diffusion model, the mean total transit time is 5.33 years with a σ of 0.99 years for all input functions. In the matrix diffusion model, the mean advective travel time is 2.55 years, with an average matrix diffusion retention time of 2.78 years. The best fit to the observed data as measured by the χ^2 residual was achieved by a dispersive age distribution with the seasonal input function developed here (Eq. 15). The observed data and the overall best fit modeled concentration for all tracers are shown in Fig. 6. Overall, the dispersion model gives the best fits to the measured data; however, the variance in χ^2 over all the precipitation input functions is high enough to encompass the χ^2 of the matrix diffusion age distribution, indicating that it is difficult to tell the difference between the two age distributions given the uncertainty in the input function (Table 4).

Table 2 summarizes the results for the V2 sampling site. The average mean travel time (τ) over all age distributions and input functions is 7.86 years with a σ of 2.2 years. For the dispersion age distribution, the average mean travel time is 10.3 with σ of 8.49. The exponential age function gives an average mean travel time of 6.06 with a σ of 2.1 years. For the matrix diffusion distribution, the mean total transit time is 7.23 years with a σ of 2.3 years, with an average mean advective travel time of 3.3 years and an average mean retention time of 3.9 years. The best fit combination of models is the dispersion age distribution

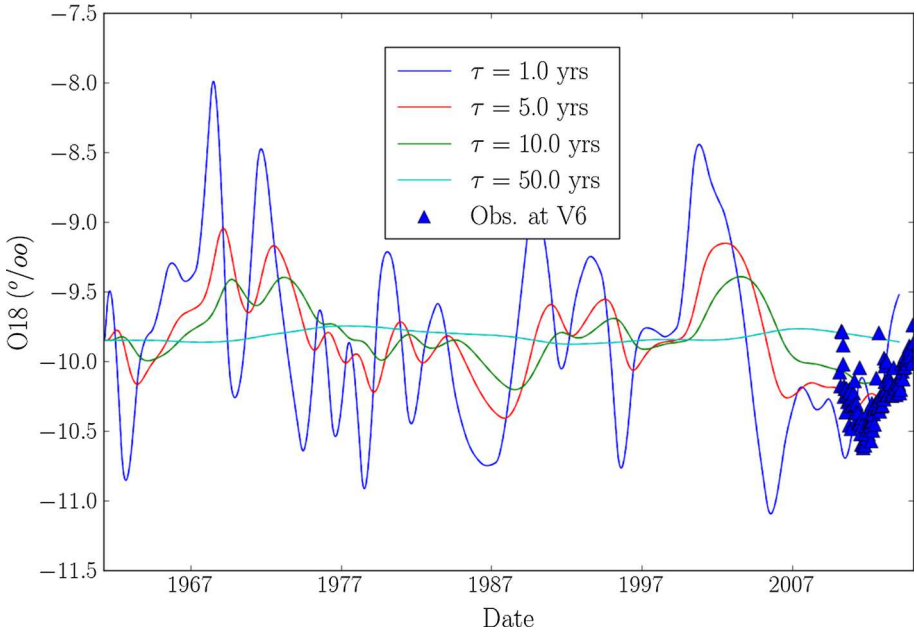

Fig. 4 Effect of increasing mean travel time on the modeled δ^{18}O signal using the annual average weighting function and the dispersion TTD for the V6 sampling site along with the observed δ^{18}O signal

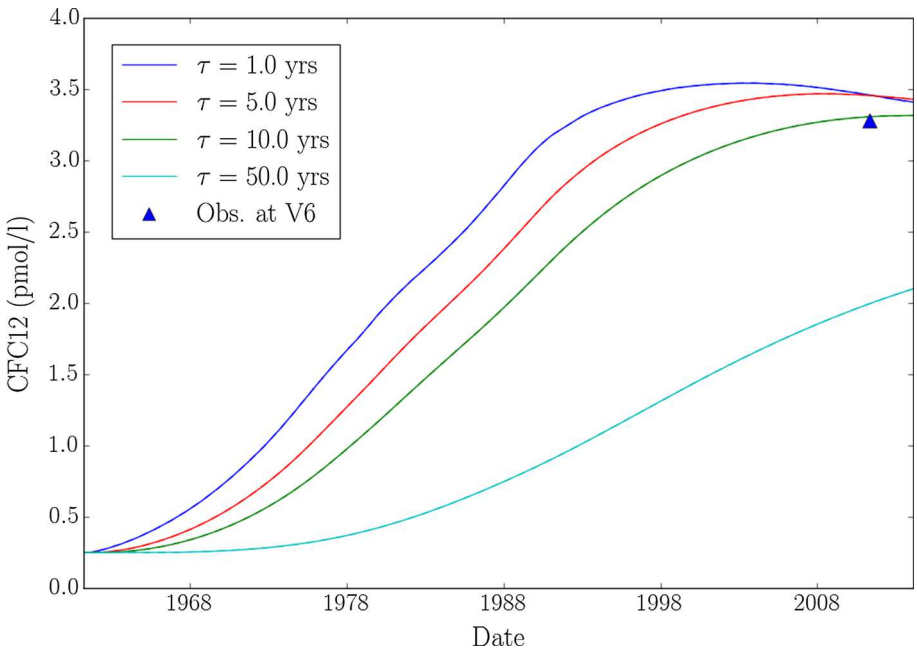

Fig. 5 Effect of increasing mean travel time on the modeled CFC-12 signal using the annual average weighting function and the dispersion TTD for the V6 sampling site along with the observed CFC concentration

and input function Eq. 15. The observed data and overall best fit modeled concentration for all tracers at V2 are shown in Fig. 7. Overall, best fits are for the dispersion model followed by the exponential and finally matrix diffusion models. The variance in χ^2 due to uncertainty in the seasonal weighting function encompasses the fits of all other travel time distributions; thus, it is difficult to uniquely pick any of the travel time distributions as the best (Table 4). For the seasonal weighting functions, the overall best fit is given by the developed seasonal weighting function (Eq. 15). This weighting function clearly provides the best fits regardless of the travel time distribution used (Table 5).

For the V4 sampling site, the overall average mean travel time is 6.56 years with σ of 1.2 years for all travel time distributions and input functions (Table 3). Average travel time for the dispersion distribution is 5.30 years with a σ of 2.13 years. Average travel time for the exponential age distribution is 6.7 years (σ 3.2 years), and average travel time for the matrix diffusion distribution is 7.74 (σ 3.2 years). For the matrix diffusion distribution, the average advective mean travel time is 3.47 years and the

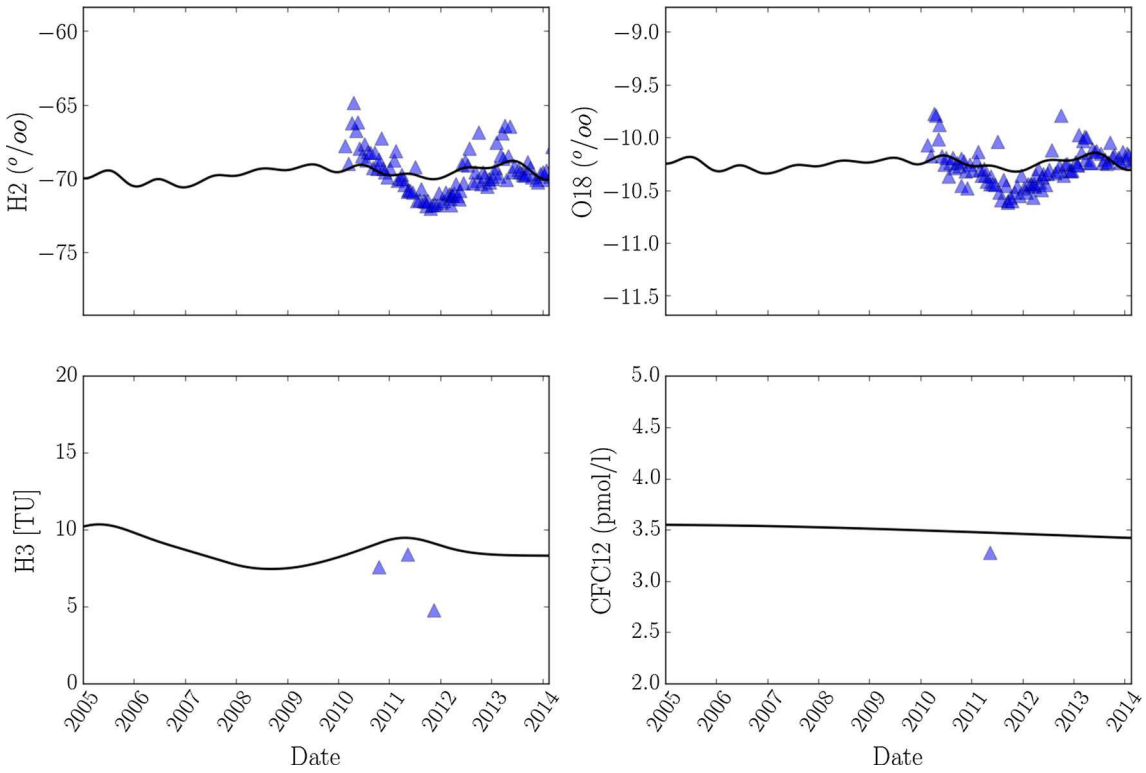

Fig. 6 Tracer data at the V6 sampling location and the overall multi-tracer best fit lumped parameter model results. For V6 the best fit was achieved for a dispersion TTD using the seasonal input function derived in Eq. 15

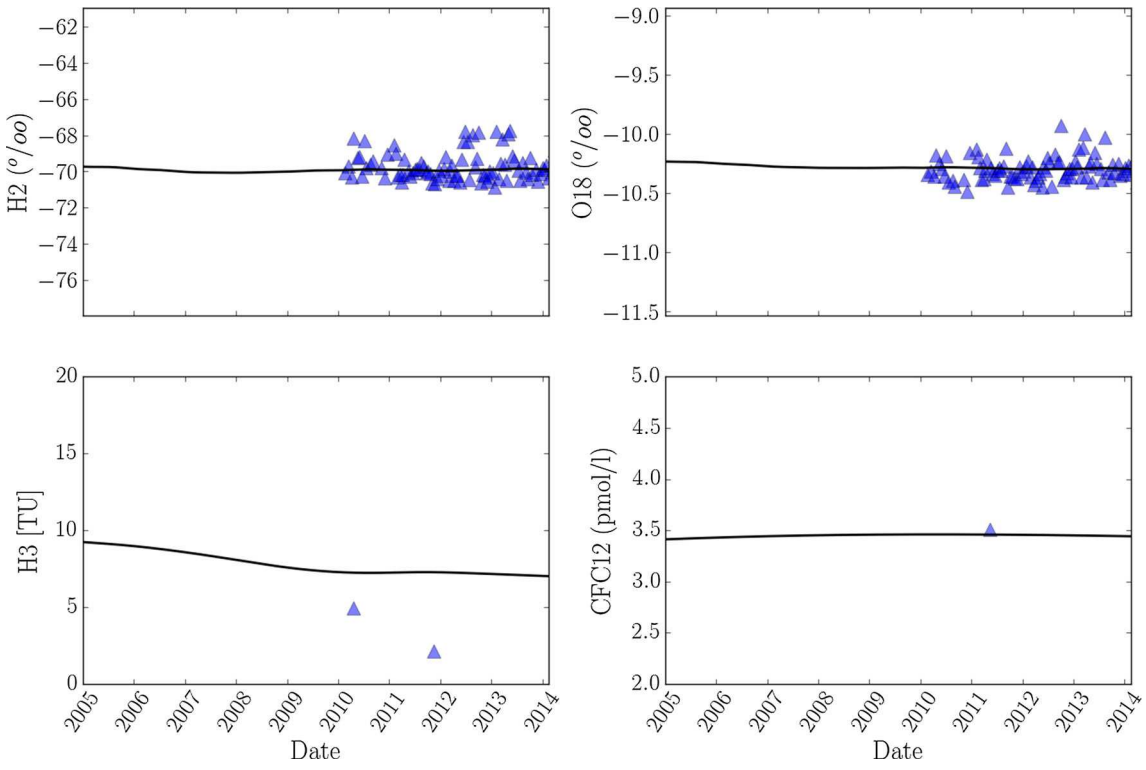

Fig. 7 Tracer data at the V2 sampling location and the overall multi-tracer best fit lumped parameter model results. For V2 the best fit was achieved for a dispersion TTD using the seasonal input function derived in Eq. 15

Table 3 Summary results for V4 sampling site

Age distribution ($g(t)$)	Infil. func. ($C_{in}(t)$)	τ_{adv} (years)	+/− (years)	χ^2	τ_{tran} years
Dispersive-Matrix Diffusion	Uniform	2.22	0.09	407	4.53
	Eq. 11	4.49	0.16	210	10.4
	Eq. 14	2.55	0.15	265	5.34
	Eq. 15	4.62	0.22	101	10.7
Dispersive	Uniform	3.27	0.18	372	
	Eq. 11	7.08	0.76	182	
	Eq. 14	7.13	0.97	242	
	Eq. 15	3.55	1.3	96.3	
Exponential	Uniform	3.15	0.18	292	
	Eq. 11	7.24	0.62	224	
	Eq. 14	5.62	0.54	271	
	Eq. 15	10.8	1.94	99.7	

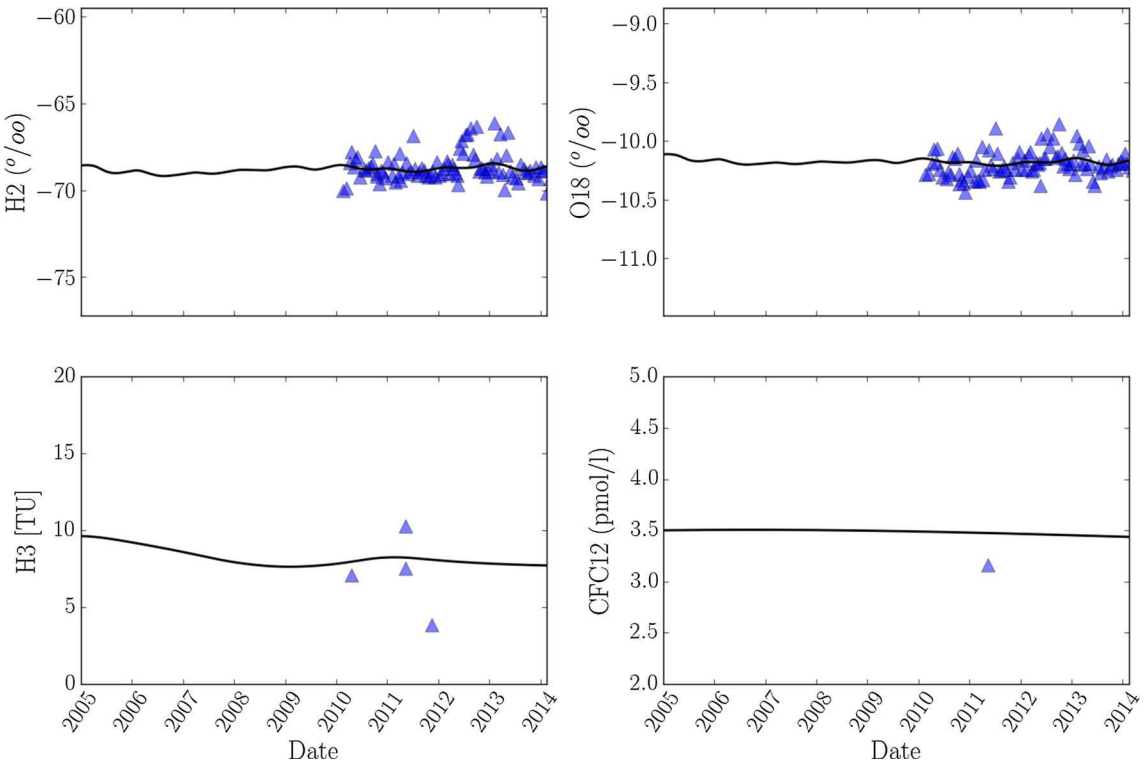

Fig. 8 Tracer data at the V4 sampling location and the overall multi-tracer best fit lumped parameter model results. For V4 the best fit was achieved for a dispersion TTD using the seasonal input function derived in Eq. 15

average retention time is 4.3 years. The best fit combination was our seasonal infiltration function (Eq. 15) with the dispersion equation; however, this combination produces an anomalously low mean travel time of 3.55 years. The observed data and overall best fit modeled concentration for all tracers at V4 are shown in Fig. 8. The exponential age distribution fits the data nearly as well with an anomalously high mean travel time of 10.8 years. Over all the seasonal weighting functions, the best fits were given by the exponential model, followed by the dispersion model and finally the matrix diffusion model. At V4, uncertainty in the input function creates enough variance in the χ^2 residual that the average χ^2 values for each TTD are within error (Table 4), thus choosing the best age distribution is difficult given the available data. As in the other models, the input function developed in this paper provides better fits than the other input functions regardless of the travel time distribution (Table 5).

Table 4 Average mean age and standard deviation of mean age estimate for all seasonal input functions given a TTD at each sample location

Model	Input func.	τ_{adv} (years)	σ (years)	$\bar{\chi}^2$	σ_χ
V6	Dispersion-matrix diffusion	5.33	0.993	328	168
	Dispersion	3.42	2.58	248	79.1
	Exponential	5	1.28	420	157
V2	Dispersion-matrix diffusion	7.24	2.31	292	201
	Dispersion	6.31	2.22	251	142
	Exponential	6.06	2.05	276	149
V4	Dispersion-matrix diffusion	7.74	3.26	246	127
	Dispersion	5.26	2.14	223	116
	Exponential	6.7	3.21	222	86.1

Table 5 Average mean age and standard deviation of mean age estimate for all TTDs given the seasonal input function at each sample location

Model	Input func.	τ_{adv} (years)	σ (years)	$\bar{\chi}^2$	σ_χ
V6	Uniform	3.49	1.09	522	160
	Eq. 11	6.49	0.78	303	22.8
	Eq. 14	4.62	1.77	270	100
	Eq. 15	3.74	2.2	231	75.1
V2	Uniform	3.86	1.31	495	69.8
	Eq. 11	8.83	1.52	214	12
	Eq. 14	6.67	0.645	275	26.6
	Eq. 15	6.82	0.17	109	2.08
V4	Uniform	3.65	0.764	357	58.9
	Eq. 11	8.23	1.85	205	21.4
	Eq. 14	6.03	0.963	259	15.3
	Eq. 15	8.36	4.17	99	2.43

Discussion

The results presented here highlight the difficulty in using tracer concentrations to constrain travel time in a fractured network system. At all sampling locations, it is difficult to distinguish the best travel time distribution when considering different conceptualizations of the seasonally weighted input function. The inability to distinguish a single best age distribution using measured tracer concentration is consistent with the findings of McCallum et al. (2014) and Solomon et al. (2010). Thus, the estimated mean age is dependent upon the conceptualization of the system. The standard error of the mean travel time estimate (defined as the standard deviation of mean travel times normalized by the average mean travel time) over all travel time distributions and seasonal weighting input functions ranges from 19 % at the V4 sampling site to 22.4 % at the V6 sampling site. These results indicate that tracer-derived mean travel times converge to a similar value consistent with Solomon et al. (2010) and can still be used to provide significant constraint on the flow system.

For two of the three model locations V6 and V2, the observed concentrations were best fit by the dispersion travel time distribution. These sampling locations correspond to the discharge from individual fractures intersecting the tunnel at different depths. The shallowest sampling location V6 had the shortest travel time, and the deeper sampling location, V2, had a longer travel time. The lumped parameter modeling is conceptually consistent with discharge from these fractures occurring a single fracture network, described a single flow path, rather a collection of multiple flow paths which mix together. For one of the locations, V4, the exponential age distribution fits the data as well as the dispersion model. At this location, discharge from a larger fault system was sampled; thus, a mixture of different flow paths with a range of ages (which the exponential model represents) is a likely conceptual model. However, uncertainty in the seasonal weighting function makes it difficult to identify which of these transit time distributions best fits the data.

The fact that the matrix diffusion model does not significantly improve fits indicates that, given the travel times in this fracture network and representative parameters controlling matrix diffusion, matrix diffusion is not a dominant process controlling transport in these fractures. The lack of significant matrix diffusion is also highlighted by the relatively small difference between the mean transport time including matrix diffusion and the mean advective only travel time (Tables 1, 2). While the effect of matrix diffusion appears small on the mean travel time in this study, we expect that matrix diffusion would play a much stronger role in controlling the initial arrival and tailing properties of the transit time distribution, which are likely not identifiable using tracer concentrations (McCallum et al. 2014). Additionally, in environments with stronger matrix diffusion (e.g., high matrix porosity and/or longer travel times), the matrix diffusion transit time distribution developed here will be useful in modeling the total transit time.

Seasonal weighting

A significant finding of this study is that the estimated mean travel time is as sensitive to the assumed seasonal input function as the travel time distribution. The effect of seasonality of recharge on the age estimate is largely unconsidered in most studies, and these results show that it is at least as important as the age distribution assumption. For isotopes of water including tritium and thus tritium–helium age dating, seasonality of recharge will always be important. Mixing of recharging waters during infiltration is a classic and active question in hydrology (e.g., Evaristo et al. 2015; Kennedy et al. 1986), and more investigation is need on the effect of seasonality on groundwater age determination. Of the seasonal recharge functions considered in this study, the developed formula consistently fits the observed data better than other functions. This function keeps the recharge concentration close to the annual average concentration, but allows large isotopic deviations in precipitation to effect the recharge concentration. While considerably more investigation is needed to validate this recharge function, the good fits here indicate that at least in this setting it appears give a reasonable approximation to the processes involved. Given the sensitivity to the infiltration weighting function, we suggest that investigators utilize more than one infiltration weighting function when using liquid-phase tracers such as stable and radiogenic isotopes of water and assess the effects of the infiltration function on their age dates. We favor the weighting function developed here as a starting point, but annual weighted precipitation may be another useful weighting function for many situations.

Vadose zone transport adds some complications for tracer comparison and seasonality of dissolved gas tracers. Stable isotopes of water and tritium are tracers of the water and thus record total transport time of water through the vadose zone and saturated zone. Dissolved gas tracers re-equilibrate with the water phase throughout the vadose zone and are finally set at the water table, thus only record saturated flow transport time. In areas of deep vadose zones, this can lead to a large discrepancy in age dates from water borne and dissolved gas tracers (Cook and Solomon 1995). However, when the vadose zone is less than 10 m, the effect is negligible (Cook and Solomon 1995). Given the physiographic setting, we expect the water table to much shallow than 10 m; thus, we assume the difference in age from water borne and dissolved gas tracers is small.

The concentration of dissolved gases is set by the physical conditions at the water table such as recharge temperature and excess air. Seasonality of recharge may not have as large an effect on travel time estimates that use dissolved gas tracers when the recharge zone is deep enough to keep the recharge temperature constant. In our simulations, we assume that the recharge temperature and therefore dissolved gas concentration are constant over the year, which means the dissolved gas tracers will not show a seasonality effect. However, in situations where the water table is shallow and seasonality is pronounced, recharge temperatures can differ from the mean annual temperature (Thoma et al. 2011) and seasonality will affect dissolved gas tracers. In these situations, the investigator must know something about the seasonal variation in temperature at the water table, which can then be used to vary the concentration of the dissolved gas tracers.

Tritium data

In all cases, the model does a relatively poor job matching the value and variance in the observed tritium concentrations and clearly highlights the inability of our model to completely describe the system. However, it is important to note that while our model is as much as 5 TU off in concentration, the overall error is relatively small variance when compared to the 4 orders of magnitude variance in historical input. The variance in tritium values is considerably higher for V2 and V4 than that of the stable isotopes. Given the stability in isotopic composition, a relatively constant tritium concentration would be expected, and all our models which attempt to fit all tracer data available produce relatively flat tritium concentrations. Some plausible explanations for the difference between the modeled and observed tritium could include transient flow (discussed below), transient binary mixing of tritium-free water and/or sampling/analytical error. We note that increased the mean age tends to increase the tritium concentration as more bomb pulse water is included, and would create a more stable tritium concentration. Given the reasonable match for other isotopes, and the fact that the analytical error for the IAEA lab is less than 1 TU, our favored cause of the mis-match is a transient flow system, which could cause the higher variation and which LPM models do not handle well.

Transient flow

Transient flow velocities are more likely in fractured systems as the groundwater storage capacity is generally low. Most LPM methods assume a constant flow field. At the Bedrichov site, discharge from the fractures was not constant. A plot of the discharge at the three modeled locations is given in Fig. 9 and reveals that variance in discharge is observable at all sampling sites, especially V2 and V6, on a roughly annual scale, with a total magnitude of less than 50 %. While this variance is not large, it still could affect the mean age estimation.

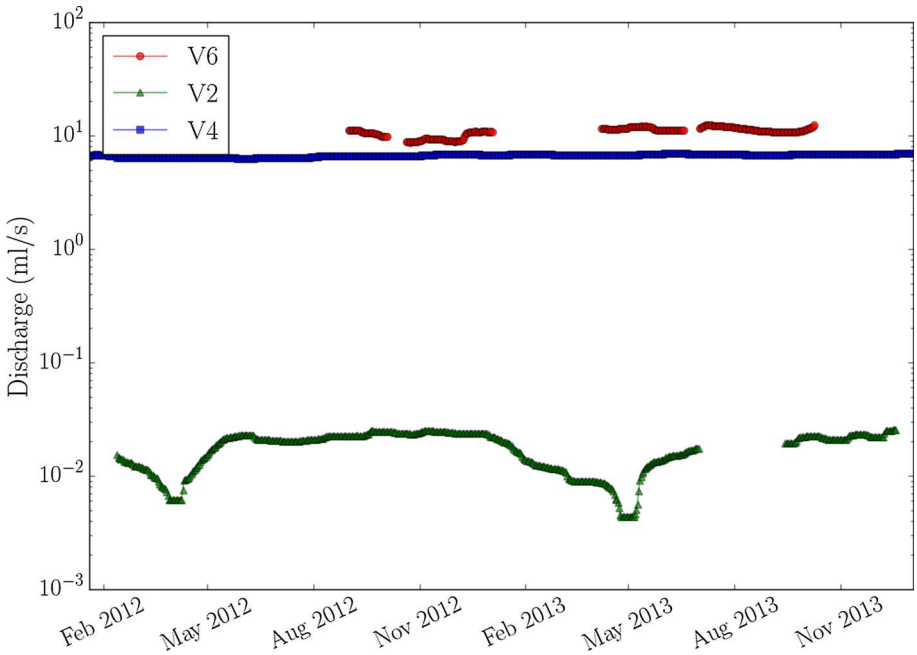

Fig. 9 Median daily discharge in ml/s measured at the V6, V2 and V4 sites by tipping gauge

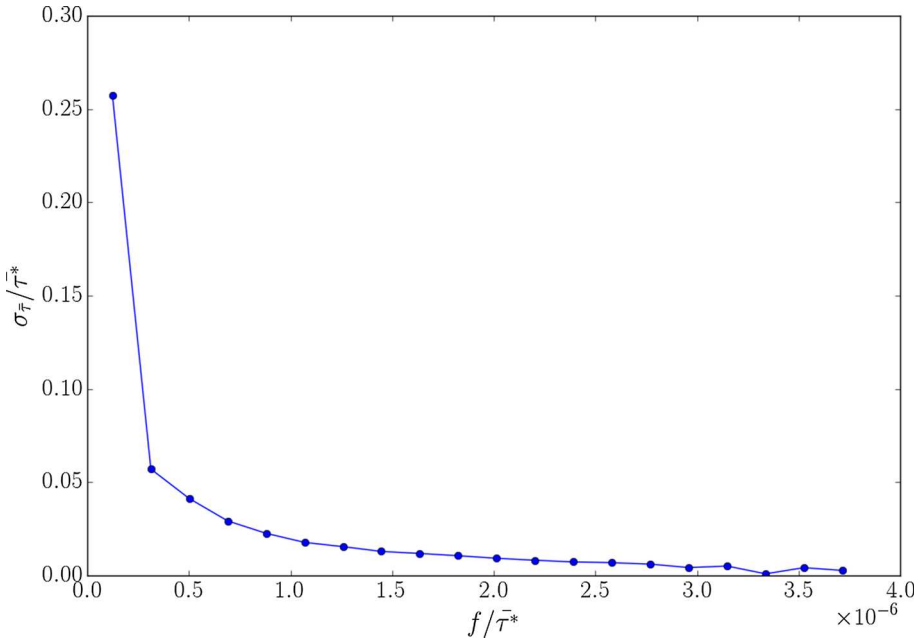

Fig. 10 Standard deviation in mean age $\sigma_{\bar{\tau}}$ as a function flow variance frequency f normalized by the steady-state travel time given the mean velocity ($\bar{\tau}^{*}$)

We investigate the effect of flow system transience by considering the effect of transient flow along a flow path, for a uniform transient velocity field $U(t) = U_o\phi(t)$, where U_o is the mean velocity and $\phi(t)$ is an arbitrary function of time which describes the velocity variance. Using the results of Soltani and Cvetkovic (2013), the cumulative travel time (τ_b) distribution under these conditions, given the location along the flow path (x), sampling time (T), inlet time (t_o) is:

$$F(\tau_b; x, T, t_o) = \frac{1}{2}\mathrm{erfc}\left[\frac{x - U_o\Phi_b(\tau_b, T)}{\sqrt{4\lambda_L U_o\Phi_b(\tau_b, T)}}\right], \tag{16}$$

where, λ_L is the longitudinal dispersion coefficient, and:

$$\Phi_b(\tau_b, T) = \int_{t_o}^{t} \phi(T - t')\mathrm{d}t'. \tag{17}$$

We set $\phi(t) = U_o + A\sin(2\pi ft)$ to simulate a periodic fluctuation in velocity of amplitude A and frequency f. The

amplitude of fluctuation was set as 50 % of U_o, which is a little greater than that observed in the data (Fig. 9). To test the effect of the flow variance, we looked at a spectrum of frequencies of flow variance. For each frequency, we performed a Monte Carlo analysis by picking 30 random starting times and calculating the cumulative age distribution, and mean age for each starting time. As a measure of the effect of variable flow, we calculate the standard deviation in calculated mean age for all starting times at a given frequency ($\sigma_{\bar{\tau}}$), normalized by the mean advective travel time using U_o alone ($\bar{\tau}^*$), for each frequency of flow variance. The results for each frequency normalized by $\bar{\tau}^*$ in Fig. 10. As long as the frequency of the variance is shorter than the mean advective travel, the observed standard deviation in mean age is less than 2 % of the advective only mean age. This implies that the mean age is fairly robust to transient flow, as long as the frequency is short compared to the overall average mean age. Given that all mean ages calculated here are greater than one year and that the observed flow variance is on a roughly annual cycle, we argue that the mean age we estimated should not be largely affected, by flow system variance.

Conclusion

In this study, we investigate the transit time distribution in fracture networks discharging to individual fractures of the Bedrichov Tunnel in the Czech Republic using time series of stable isotopes of water and tritium along with synoptic dissolved CFC concentrations. We use lumped parameter models to compare some likely transit time distributions and determine the effect of transit time distribution and seasonal input choice on the estimated mean age. We compare residence time distribution for a single advective path with longitudinal dispersion, complete mixing (exponential age distribution) and a newly developed a residence time distribution for 1D advective–dispersive transport with infinite matrix diffusion. In order to investigate the effect of seasonal recharge, we compare uniform infiltration, a weighting function developed in Zuber and Maloszewski (2001) and a weighting function developed in this paper. We find that the modeled concentrations are dependent upon the transit time distribution and the seasonal infiltration weighting function and that the estimated mean travel time is as sensitive to the choice of seasonal weighting function as that of the transit time distribution. Given the uncertainty in the seasonal weighting function, it is difficult to completely identify the best fit transit time distribution. However, regardless of the age distribution or the infiltration model chosen, the best fit mean age converges to a similar value for all three locations modeled here. These results indicate that lumped parameter models along with multiple environmental tracers can be used to constrain the mean age, and develop some information on the transit time distribution to help develop conceptual models of flow and transport in fracture networks. The results and methods presented should be applicable in other fractured crystalline environments.

Acknowledgments The work described in this paper was conducted within the context of the international DECOVALEX 2015 Project. The authors are grateful to the funding organizations who supported the work. The views expressed in the paper are, however, those of the authors and are not necessarily those of the funding organizations. Technical University of Liberec (TUL) has been supported by the Radioactive Waste Repository Authority of the Czech Republic (SURAO), under contract No. SO2013-077. The results of the TUL authors were also obtained through the financial support of the Ministry of Education of the Czech Republic (MSMT) from the project LO1201 in the framework of the targeted support of the "National Programme for Sustainability I." BGR's work was supported by the BMWi (Bundesministerium fur Wirtschaft und Energie, Berlin). Sandia National Laboratory was supported under the DOE-Used Fuel Disposition campaign. Sandia National Laboratories is a multi-program laboratory managed and operated by Sandia Corporation, a wholly owned subsidiary of Lockheed Martin Corporation, for the US Department of Energy's National Nuclear Security Administration under contract DE-AC04-94AL85000.

References

Bullister JL (2011) Atmospheric CFC-11, CFC-12, CFC-113, CCl4 and SF6 histories. Tech. rep., Carbon Dioxide Information Analysis Center, Oak Ridge National Laboratory, US Department of Energy, Oak Ridge. http://cdiac.ornl.gov/ftp/oceans/CFC_ATM_Hist/

Cook PG, Solomon DK (1995) Transport of atmospheric trace gases to the water table. Implications for groundwater dating with chlorofluorocarbons and krypton 85. Water Resour Res 31(2):263–270

Cook P, Herczeg AL (2000) Environmental tracers in subsurface hydrology. Kluwer Academic, Norwell

Cook P, Robinson N (2002) Estimating groundwater recharge in fractured rock from environmental H-3 and Cl-36. Water Resour Res. doi:10.1029/2001WR000772

Cook P, Love A, Robinson N, Simmons C (2005) Groundwater ages in fractured rock aquifers. J Hydrol 308(1–4):284–301. doi:10.1016/j.jhydrol.2004.11.005

Danckwerts P (1953) Continuous flow systems. Chem Eng Sci 2(1):1–13. doi:10.1016/0009-2509(53)80001-1

Doyon B, Molson JW (2012) Groundwater age in fractured porous media: analytical solution for parallel fractures. Adv Water Resour 37:127–135. doi:10.1016/j.advwatres.2011.11.008

Evaristo J, Jasechko S, McDonnell JJ (2015) Global separation of plant transpiration from groundwater and streamflow. Nature 525(7567):91–94. doi:10.1038/nature14983

Gardner WP, Susong DD, Solomon DK, Heasler HP (2010) Snowmelt hydrograph interpretation: revealing watershed scale hydrologic characteristics of the Yellowstone volcanic plateau. J Hydrol 383(3–4):209–222. doi:10.1016/j.jhydrol.2009.12.037

Gardner WP, Susong DD, Solomon DK, Heasler HP (2011) A multitracer approach for characterizing interactions between

shallow groundwater and the hydrothermal system in the Norris Geyser Basin area, Yellowstone National Park. Geochem Geophys Geosyst 12(8):Q08005. doi:10.1029/2010GC003353

Grabczak J, Ròzański K, Maloszewski P, Zuber A (1984) Estimation of the tritium input function with the aid of stable isotopes. Catena 11(2):105–114. doi:10.1016/0341-8162(84)90001-8

Haggerty R, Gorelick SM (1995) Multiple-rate mass transfer for modeling diffusion and surface reactions in media with pore-scale heterogeneity. Water Resour Res 31(10):2383–2400. doi:10.1029/95WR10583

Haggerty R, McKenna SA, Meigs LC (2000) On the late-time behavior of tracer test breakthrough curves. Water Resour Res 36(12):3467–3479. doi:10.1029/2000WR900214

Haggerty R, Fleming SW, Meigs LC, McKenna SA (2001) Tracer tests in a fractured dolomite: 2. Analysis of mass transfer in single-well injection-withdrawal tests. Water Resour Res 37(5):1129–1142. doi:10.1029/2000WR900334

Kennedy V, Kendall C, Zellweger G, Wyerman T, Avanzino R (1986) Determination of the components of stormflow using water chemistry and environmental isotopes, Mattole River basin, California. J Hydrol 84(12):107–140. doi:10.1016/0022-1694(86)90047-8

Klomínský J, Woller Fe (2010) Geological studies in the Bedrichov water supply tunnel. RARWRA technical report 02/20 10, Czech Geological Survey, Prague

Maloszewski P, Zuber A (1982) Determining the turnover time of groundwater systems with the aid of environmental tracers. J Hydrol 57(3):207–231. doi:10.1016/0022-1694(82)90147-0

Maloszewski P, Zuber A (1985) On the theory of tracer experiments in fissured rocks with a porous matrix. J Hydrol 79(3):333–358. doi:10.1016/0022-1694(85)90064-2

Maloszewski P, Zuber A (1990) Mathematical modeling of tracer behavior in short-term experiments in fissured rocks. Water Resour Res 26(7):1517–1528. doi:10.1029/WR026i007p01517

Maloszewski P, Zuber A (1996) Lumped parameter models for the interpretation of environmental tracer data. IAEA technical report

McCallum JL, Engdahl NB, Ginn TR, Cook PG (2014) Nonparametric estimation of groundwater residence time distributions: What can environmental tracer data tell us about groundwater residence time? Water Resour Res. doi:10.1002/2013WR014974

Neretnieks I (1980) Diffusion in the rock matrix: an important factor in radionuclide retardation? J Geophys Res Solid Earth 85(B8):4379–4397. doi:10.1029/JB085iB08p04379

Neretnieks I (1981) Age dating of groundwater in fissured rock: influence of water volume in micropores. Water Resour Res 17(2):421–422. doi:10.1029/WR017i002p00421

Neuman S (2005) Trends, prospects and challenges in quantifying flow and transport through fractured rocks. Hydrogeol J 13(1):124–147. doi:10.1007/s10040-004-0397-2

Painter S, Cvetkovic V (2005) Upscaling discrete fracture network simulations: an alternative to continuum transport models. Water Resour Res 41(2):W02002. doi:10.1029/2004WR003682

Painter S, Cvetkovic V, Mancillas J, Pensado O (2008) Time domain particle tracking methods for simulating transport with retention and first-order transformation. Water Resour Res 44(1):W01406. doi:10.1029/2007WR005944

Penna D, Stenni B, Šanda M, Wrede S, Bogaard TA, Gobbi A, Borga M, Fischer BMC, Bonazza M, Chárová Z (2010) On the reproducibility and repeatability of laser absorption spectroscopy measurements for δ^2h and δ^{18}o isotopic analysis. Hydrol Earth Syst Sci 14(8):1551–1566. doi:10.5194/hess-14-1551-2010

Rálek P, Hokr M (2013) Methods of water inflow measurement in the bedrichov tunnel. Explor Geophys Remote Sens Environ 2:30–39

Roubinet D, de Dreuzy JR, Tartakovsky DM (2013) Particle-tracking simulations of anomalous transport in hierarchically fractured rocks. Comput Geosci 50:52–58. doi:10.1016/j.cageo.2012.07.032

Šanda M, Vitvar T, Kulasová A, Jankovec J, Císlerová M (2014) Run-off formation in a humid, temperate headwater catchment using a combined hydrological, hydrochemical and isotopic approach (Jizera Mountains, Czech Republic). Hydrol Process 28(8):3217–3229. doi:10.1002/hyp.9847

Shapiro AM (2001) Effective matrix diffusion in kilometer-scale transport in fractured crystalline rock. Water Resour Res 37(3):507–522. doi:10.1029/2000WR900301

Solomon DK, Genereux DP, Plummer LN, Busenberg E (2010) Testing mixing models of old and young groundwater in a tropical lowland rain forest with environmental tracers. Water Resour Res 46(4):W04518. doi:10.1029/2009WR008341

Solomon DK, Gilmore TE, Solder JE, Kimball B, Genereux DP (2015) Evaluating an unconfined aquifer by analysis of age-dating tracers in stream water. Water Resour Res 51(11):8883–8899. doi:10.1002/2015WR017602

Soltani SS, Cvetkovic V (2013) On the distribution of water age along hydrological pathways with transient flow. Water Resour Res 49(9):5238–5245. doi:10.1002/wrcr.20402

Sudicky EA, Frind EO (1982) Contaminant transport in fractured porous media: analytical solutions for a system of parallel fractures. Water Resour Res 18(6):1634–1642. doi:10.1029/WR018i006p01634

Tang DH, Frind EO, Sudicky EA (1981) Contaminant transport in fractured porous media: analytical solution for a single fracture. Water Resour Res 17(3):555–564. doi:10.1029/WR017i003p00555

Therrien R, Sudicky E (1996) Three-dimensional analysis of variably-saturated flow and solute transport in discretely-fractured porous media. J Contam Hydrol 23(1–2):1–44. doi:10.1016/0169-7722(95)00088-7

Thoma MJ, McNamara JP, Gribb MM, Benner SG (2011) Seasonal recharge components in an urban/agricultural mountain front aquifer system using noble gas thermometry. J Hydrol 409(12):118–127. doi:10.1016/j.jhydrol.2011.08.003

Warren JE, Root PJ (1963) The behavior of naturally fractured reservoirs. Soc Petro Eng J 3(03):245–255

Weiss R (1968) Piggyback sampler for dissolved gas studies on sealed water samples. Deep Sea Research and Oceanographic Abstracts, vol 15, no. 6, pp 695–699

Zak J, Verner K, Klominsky J, Chlupacova M (2009) "Granite tectonics" revisited: insights from comparison of K-feldspar shape-fabric, anisotropy of magnetic susceptibility (AMS), and brittle fractures in the Jizera granite, Bohemian Massif. Int J Earth Sci 98(5):949–967

Zuber A, Maloszewski P Yurtseveir Y (eds) (2001) Environmental isotopes in the hydrologic cycle, vol 6. International atomic energy agency